EJECTA PATTERNS OF METEOR CRATER, ARIZONA DERIVED FROM THE LINEAR UN-MIXING OF TIMS DATA AND LABORATORY THERMAL EMISSION SPECTRA

Michael S. Ramsey and Philip R. Christensen

Department of Geology, Arizona State University
Tempe, Arizona 85287-1404

1. INTRODUCTION

Accurate interpretation of thermal infrared data depends upon the understanding and removal of complicating effects. These effects may include physical mixing of various mineralogies and particle sizes, atmospheric absorption and emission, surficial coatings, geometry effects and differential surface temperatures. The focus of this study is the examination of the linear spectral mixing of individual mineral or endmember spectra. Linear addition of spectra, for particles larger than the wavelength *(Salisbury et al, 1987)*, allows for a straight-forward method of deconvolving the observed spectra, predicting a volume percent of each endmember. The 'forward analysis' of linear mixing (comparing the spectra of physical mixtures to numerical mixtures) has received much attention *(Thomson & Salisbury 1991; Christensen et al, 1986)*. The reverse approach of un-mixing thermal emission spectra has been examined with remotely sensed data *(Adams et al, 1989; Gillespie et al, 1990)*, but no laboratory verification exists. Understanding of the effects of spectral mixing on high resolution laboratory spectra allows for the extrapolation to lower resolution, and often more complicated, remotely gathered data.

Thermal Infrared Multispectral Scanner (TIMS) data for Meteor Crater, Arizona were acquired in September, 1987. The spectral un-mixing of these data gives a unique test of the laboratory results. Meteor Crater (1.2 km in diameter and 180 m deep) is located in north-central Arizona, west of Canyon Diablo *(Shoemaker & Kieffer, 1974)*. The arid environment, paucity of vegetation and low relief make the region ideal for remote data acquisition. Within the horizontal sedimentary sequence that forms the upper Colorado Plateau, the oldest unit sampled by the impact crater was the Permian Coconino Sandstone. A thin bed of the Toroweap Formation, also of Permian age, conformably overlays the Coconino. Above the Toroweap lies the Permian Kiabab Limestone which, in turn, is covered by a thin veneer of the Moenkopi Formation. The Moenkopi is Triassic in age and has two distinct sub-units in the vicinity of the crater. The lower, Wupatki member, is a fine-grained sandstone, while the upper, Moqui member, is a fissile siltstone *(Shoemaker & Kieffer, 1974)*. Ejecta from these units are preserved as inverted stratigraphy up to 2 crater radii from the rim. The mineralogical contrast between the units, relative lack of post-emplacement erosion *(Grant & Schultz, 1989)* and ejecta mixing provide a unique site to apply the un-mixing model. Selection of the aforementioned units as endmembers reveals distinct patterns in the ejecta of the crater.

2. LABORATORY SPECTRA

Particles between 355 and 500μm were used to reduce the effects of volume scattering; the choice of endmember minerals approximates the mixing of Kiabab Limestone and Coconino Sandstone in the crater ejecta. Laboratory thermal emission spectra (Fig. 1) of the powders were acquired on a Mattson Cygnus 100 FTIR interferometer/spectrometer. Absolute emissivity was obtained using the technique described by *(Christensen & Harrison, 1992)*. The endmember components, mixed by volume into binary mixtures, were agitated after each of the five spectral acquisitions. This process assured accurate spectral sampling and charted the daily variation of the spectrometer, which varied by less than 1% absolute emissivity. The five runs were then averaged to produce a final spectrum. The calcite endmember spectra shows the characteristic absorption band associated with the vibration of the carbonate ion (≈1550 cm^{-1}) and the large reststrahlen band produced by the Si-O bending mode of quartz (≈1150 cm^{-1}) *(Salisbury et al, 1987)*.

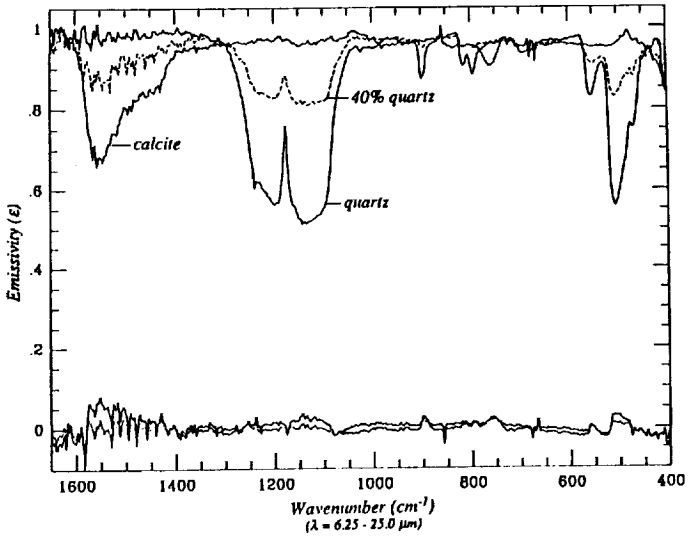

FIG. 1. Emission spectra of 355-500μm quartz and calcite. The dashed line shows the physical mixture of 40% quartz, 60% calcite. Errors (Δε) in the model fit for the 40% quartz mixture are shown in the bottom curves. The solid line is the two endmember case, while the dotted line indicates the improved error after blackbody correction.

The spectra of the two endmembers were used as reference inputs to the model. A least-squares fit of the data results in the percentage of each endmember as well as the "goodness-of-fit" of the model to the data (rms error) *(Adams et al, 1989; Gillespie et al, 1990)*. Figure 2 shows the results for the quartz endmember. Predicted percentages were within *8%* of actual values and validate the linear assumption for particles larger than the wavelength. The largest rms errors (Fig. 1) occur over the strong absorption features, and are due to a band shallowing in the spectra of the physical mixtures. The behavior over these regions, a function of the photon path length and the imaginary part of the index of refraction k(λ), appears to be slightly non-linear. The use of unimodal grain sizes virtually eliminates a change in the path length, indicating the non-linear behavior must be related to the change in the overall k(λ) of the mixture. The band shallowing can be approximated by the addition of blackbody emissivity *(Ramsey & Christensen, 1992)*.

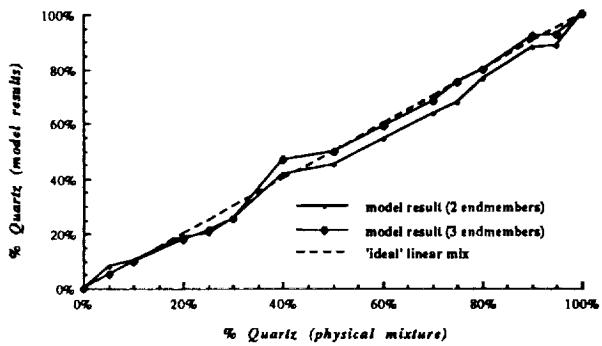

FIG. 2. Model predicted results for the percentage of quartz. Squares indicate the values obtained using two endmembers; the diamonds show the improved results using blackbody emissivity as a third endmember.

Using a constant emissivity of 1.0 as a third endmember improved the results to better than *5%*, reducing the errors over the bands. The model, re-run on the lab spectra convolved to TIMS resolution, predicted the percentages to within *10%*; however, no attempt was made to model the effect of additional noise.

3. METEOR CRATER IMAGE ANALYSIS

Standard image enhancement techniques such as the decorrelation stretch do not account for large temperature differentials within the scene and tend to stretch microphonic noise as well. A spectral un-mixing analysis eliminates these problems, however. For this study, six emissivity images were extracted from the TIMS data using the spectrum normalization technique *(Realmuto, 1990)*. An improvement in the algorithm allows for interactive linear stretching of the emissivity images for a maximum spectral contrast prior to input into the un-mixing program. The aforementioned stratigraphic units were used as endmembers for the model (5 total). These endmembers accurately fit the data to within ± 2 DN except for areas over the buildings and road. The Coconino endmember image clearly reveals a NE trending windstreak *(Grant & Schultz, 1989)*, which is a thin (<50 cm) veneer of eolian-derived material. In addition, subtle patterns within the Kiabab indicate the true extent of the ejecta. This supports the interpretation of *(Grant & Schultz, 1989)* who state that the ejecta is well-preserved below the thin alluvial mantling deposits derived from Holocene erosion. These patterns are not evident in the decorrelation stretched image and must be field verified. Differentiation of slight mineralogical changes within the Moenkopi are also clearly distinguished and allow for improved eject mapping.

4. REFERENCES

Adams, J.B., M.O. Smith, and A.R. Gillespie, Simple models for complex natural surfaces: a strategy for the hyperspectral era of remote sensing, in *Proc. IEEE Intl. Geosci. & Remote Sensing Symp.*, 16-21, 1989.

Christensen, P.R., H.H. Kieffer, S.C. Chase, D.D. Laporte, A thermal emission spectrometer for identification of surface composition from earth orbit, in *Commercial applications and scientific research requirements for thermal infrared observations of terrestrial surfaces, NASA-EOSAT Joint Report*, 119-132, 1986.

Christensen, P.R. and S.T. Harrison, Thermal-infrared emission spectroscopy of natural surfaces: application to desert varnish coatings on rocks, to be submitted to - *J. Geophys. Res.*, 1992.

Gillespie, A.R., M.O. Smith, J.B. Adams and S.C. Willis, Spectral mixture analysis of multispectral thermal infrared images, in *Abbott, E.A. (Ed.), Proc. of the Second TIMS Workshop, JPL Pub. 90-55*, JPL, Pasadena, Calif., 57- 74, 1990.

Grant, J.A. and P.H. Schultz, The erosional state and style of Meteor Crater, Arizona, *Lunar and Planet. Sci. XX*, 355-356, 1989.

Ramsey, M.S. and P.R. Christensen, The linear "un-mixing" of laboratory infrared spectra: implications for the thermal infrared emission spectrometer (TES) experiment, Mars Observer, *Lunar and Planet. Sci. XXIII*, 1127-1128, 1992.

Realmuto, V.J., Separating the effects of temperature and emissivity: emissivity spectrum normalization, in *Abbott, E.A. (Ed.), Proc. of the Second TIMS Workshop, JPL Pub. 90-55*, JPL, Pasadena, Calif., 26-30, 1990.

Salisbury, J.W., B. Hapke, and J.W. Eastes, Usefulness of weak bands in the midinfrared remote sensing of particulate planetary surfaces, *J. Geophys. Res. 92*, 702-710, 1987.

Shoemaker, E.M. and S.E. Kieffer, Guidebook to the geology of Meteor Crater, Arizona: *ASU Center for Meteorite Studies Publication 17*, Tempe, Arizona, 66p, 1974.

Thomson, J.W. and J.W. Salisbury, The mid-infrared reflectance of mineral mixtures (7-14 μm), submitted - *Remote Sensing of the Enviro.*, 1991.